



Real-time GFP imaging of spontaneous HT-1080 fibrosarcoma lung metastases

Norio Yamamoto^{1–3}, Meng Yang¹, Ping Jiang¹, Hiroyuki Tsuchiya³, Katsuro Tomita³, A.R. Moossa² & Robert M. Hoffman^{1,2}

¹AntiCancer, Inc., San Diego, California, USA; ²Department of Surgery, University of California, San Diego, California, USA; ³Department of Orthopedic Surgery, School of Medicine, Kanazawa University, Kanazawa, Ishikawa, Japan

Received 21 August 2002; accepted in revised form 11 November 2002

Key words: green fluorescent protein, lung metastasis, optical imaging, skin-flap window

Abstract

Metastasis to the lung is often a lethal event in sarcoma as well as other cancers. We report here a new animal model of sarcoma enabling the external real-time fluorescence imaging of spontaneous lung metastasis. The human fibrosarcoma cell line HT-1080 was transduced with the green fluorescent protein (GFP) gene. HT-1080-GFP cells were injected into the right hind footpad of severe combined immunodeficient (SCID) mice. The lung metastases were evaluated by whole-body fluorescence imaging as well as direct-view imaging in live animals through a skin-flap window over the chest wall. Spontaneous lung metastases were observed on the lungs of 11 of 12 mice. SCID mice well tolerated the skin-flap procedure enabling real-time imaging of spontaneous lung metastases with a resolution of approximately 50–100 μm . This procedure enabled external imaging at the micrometastasis level. Real-time evaluation of spontaneous lung metastasis in the same animals should allow drug evaluation and mechanistic studies not previously possible.

Introduction

Lung metastasis is the major cause of mortality in bone and soft tissue sarcomas [1–3]. In classical animal models of human sarcoma, evaluation of lung metastasis is made by sacrifice of animals at each time point [4], precluding real-time visualization of metastasis formation and behavior in the living animal.

Our previous studies have shown that green fluorescent protein (GFP) enables visualization of tumor cells in fresh tissue [5–11]. We have recently shown that GFP enables whole-body imaging of tumors and their metastases in live animals in real time [12, 13]. In the present study, we have transduced the HT-1080 human fibrosarcoma cell line with GFP and were able to externally image lung metastasis formation and growth in real time.

Materials and methods

Production of GFP retrovirus

The pLEIN retroviral vector (CLONTECH Laboratories, Inc., Palo Alto, California) expressing enhanced green fluorescent protein (EGFP) and the neomycin resistance gene on the same bicistronic message was used as a GFP expression vector [14]. PT67, an NIH3T3-derived packaging

cell line, expressing the 10 A1 viral envelope, was purchased from CLONTECH Laboratories, Inc. PT67 cells were cultured in DME medium (Irvine Scientific, Santa Ana, California) supplemented with 10% heat-inactivated fetal bovine serum (FBS) (Gemini Bio-products, Calabasas, California). For vector production, packaging cells (PT67), at 70% confluence, were incubated with a precipitated mixture of DOTAPTM reagent (Boehringer Mannheim, Indianapolis, Indiana), and saturating amounts of pLEIN plasmid for 18 h. Fresh medium was replenished at this time. The cells were examined by fluorescence microscopy 48 h post-transduction. For selection, the cells were cultured in the presence of 500–2,000 $\mu\text{g/ml}$ of G418 (Life Technologies, Grand Island, New York) for seven days to select for a clone producing high amounts of a GFP retroviral vector (PT67-GFP).

GFP gene transduction of fibrosarcoma cells

For GFP gene transduction, 70% confluent HT-1080 cells were incubated with a 1:1 precipitated mixture of retroviral supernatants of PT67-GFP cells and RPMI 1640 (Mediatech, Inc., Herndon, Virginia) containing 10% fetal bovine serum for 72 h. Fresh medium was replenished at this time. Cells were harvested by trypsin/EDTA 72 h post-transduction and subcultured at a ratio of 1:15 into selective medium, which contained 200 $\mu\text{g/ml}$ of G418. The level of G418 was increased stepwise up to 800 $\mu\text{g/ml}$. Clones of HT-1080 expressing high levels of GFP were isolated with cloning cylinders (Bel-Art Products, Pequannock, New

Correspondence to: Robert M. Hoffman, PhD, AntiCancer, Inc., 7917 Ostrow Street, San Diego, CA 92111, USA. Tel: +1-858-654-2555; Fax: +1-858-268-4175; E-mail: all@anticancer.com

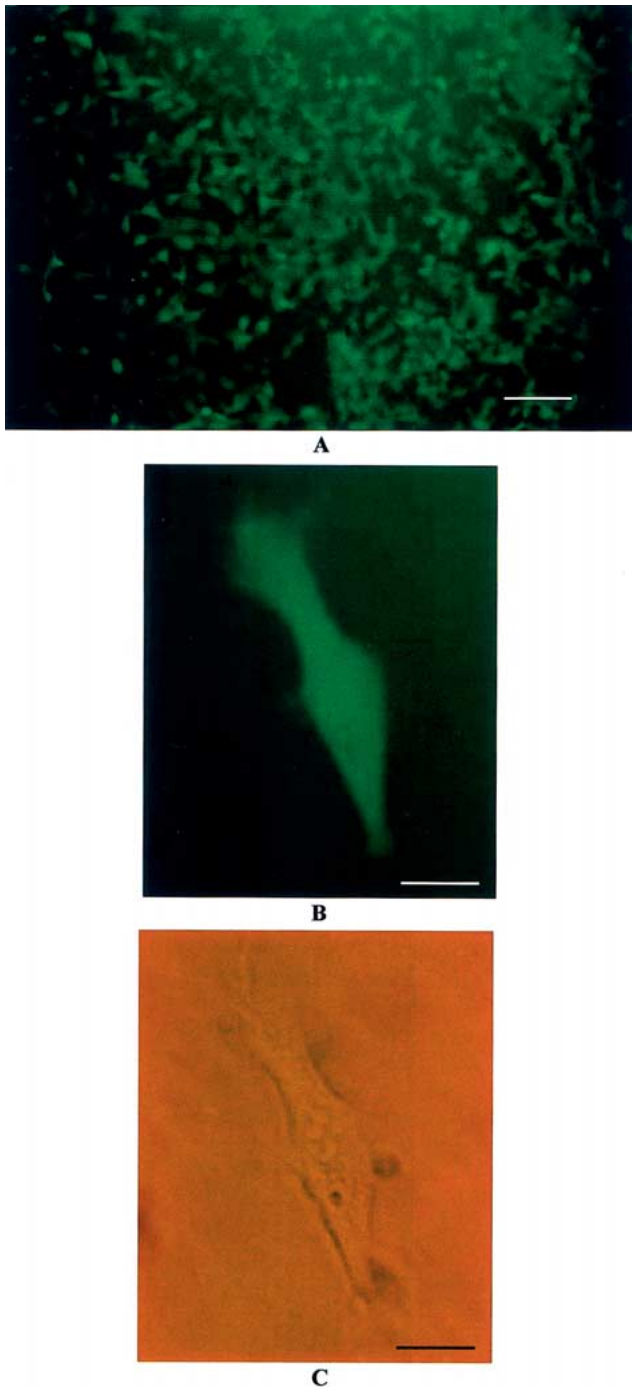
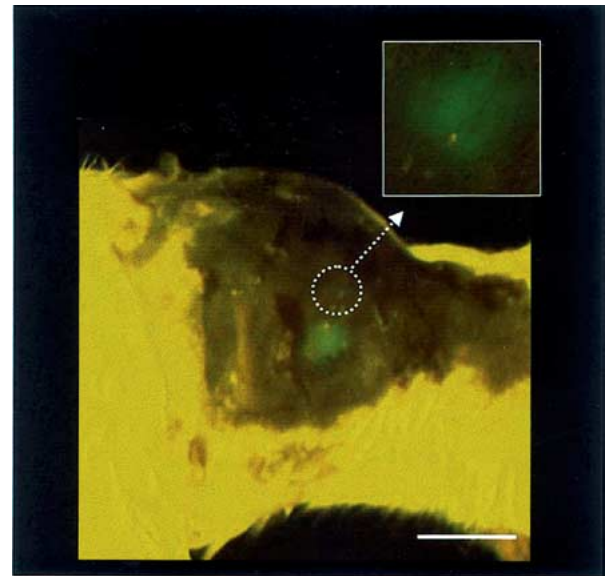


Figure 1. Stable high GFP-expressing human fibrosarcoma cells (HT-1080-GFP) in low magnification view *in vitro*. (A) Human fibrosarcoma cells (HT-1080) were transduced with GFP and the neomycin resistance gene in a retrovirus vector. High GFP-expressing cells were selected with G418 up to 800 $\mu\text{g/ml}$. Please see 'Materials and methods' for details. Bar, 500 μm . (B) Fluorescent image. (C) Bright-field image. Bar, 50 μm .

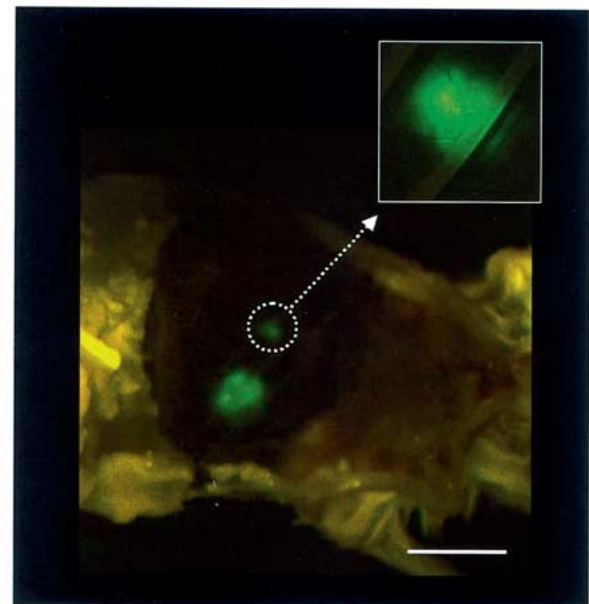
Jersey) using trypsin/EDTA and amplified by conventional culture methods.

Doubling time of stable GFP clones

GFP transduced or nontransduced parental cells were seeded at 1.5×10^4 in 35-mm culture dishes. The cells were harvested and counted every 24 h using a hemocytometer



A



B

Figure 2. External images of lung metastases of HT-1080-GFP cells in a living mouse. (A) Whole-body images of lung metastases were captured through the skin after hair removal. Metastases were visualized through the skin by bright GFP fluorescence. Close-up view ($\times 8$) is indicated in white square. (B) External images were captured through the chest wall via a skin-flap window. Lung metastasis was visualized more clearly with the skin-flap window than with imaging through skin. Close-up view ($\times 10$) is indicated in white square. Bars, 10 mm.

(Reichert Scientific Instruments, Buffalo, New York). The doubling time was calculated from the cell-growth curve over six days.

Time course external imaging of spontaneous lung metastases in living mice

To obtain time-course images of spontaneous lung metastases, four-week-old female SCID mice were first injected with 5×10^6 HT-1080-GFP cells in the right hind footpad.

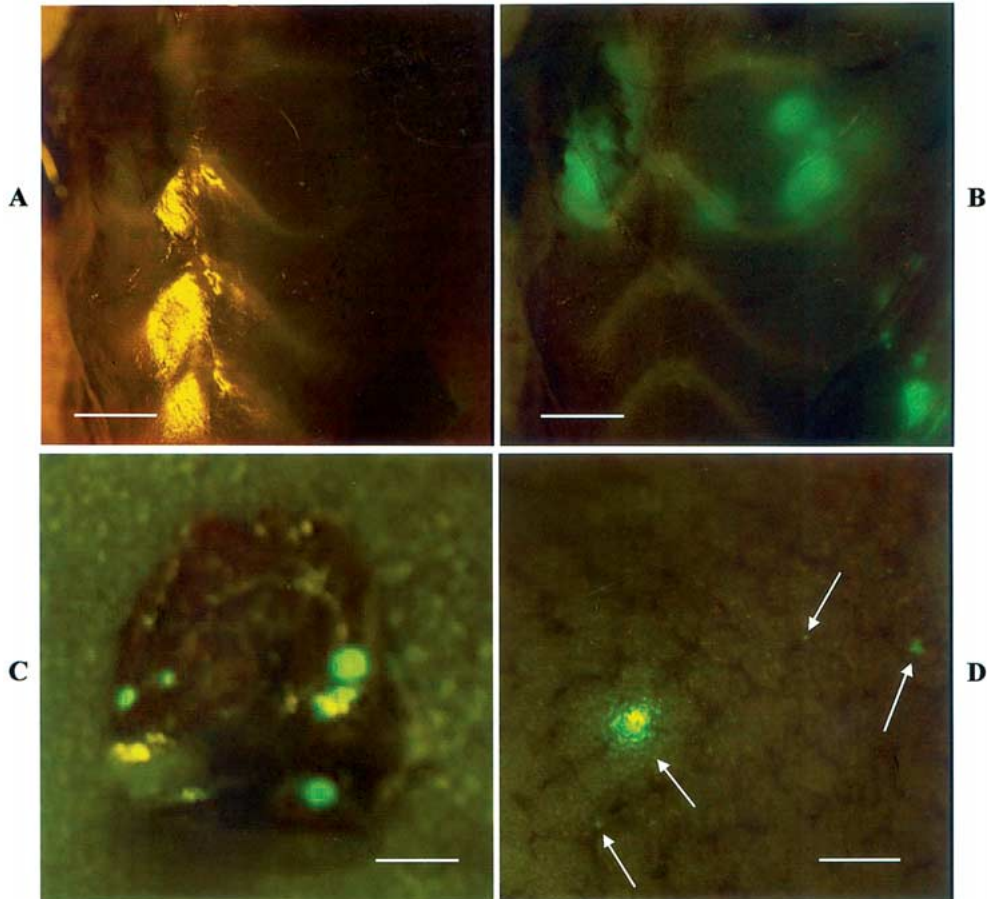


Figure 3. External light and fluorescent images of lung metastases at autopsy. (A) With bright-field imaging, metastasis could not be detected. (B) With fluorescence imaging, small metastases of varying sizes could be detected on the lung. (C) After sacrifice, the lungs were removed and the number of lung metastatic colonies were counted under 2× magnification with a CCD camera. Bars, 7.5 mm. (D) To evaluate micrometastases, extracted lungs were observed under fluorescence microscopy. Micrometastases, at the single-cell level, could be visualized by GFP expression in the lung. White arrows indicate micrometastases. Bar, 300 μm.

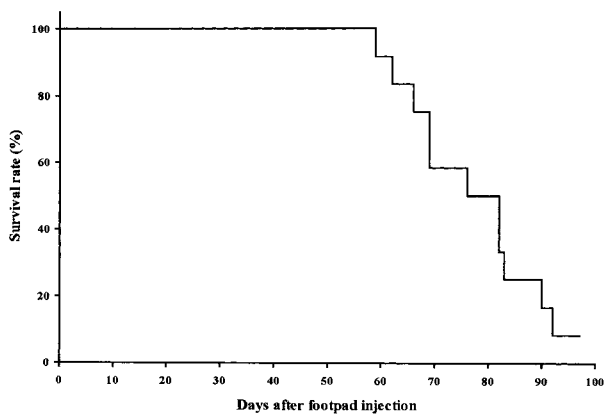


Figure 4. Survival rate of mice after footpad injection of HT-1080-GFP cells. Almost all mice survived from 60–90 days after footpad injection. See ‘Materials and methods’ for details.

→
Figure 5. Time-course images of lung micrometastasis in a living mouse. (A) Micrometastases were observed with fluorescent microscopy via a skin-flap window beginning eight weeks after footpad injection (day 56). See ‘Materials and methods’ for details. Bars, 500 μm. (B) Micrometastasis area was calculated assuming an elliptical shape using the equation below: $S \text{ (area)} = 3.14 \times (\text{long diameter}) \times (\text{short diameter})$.

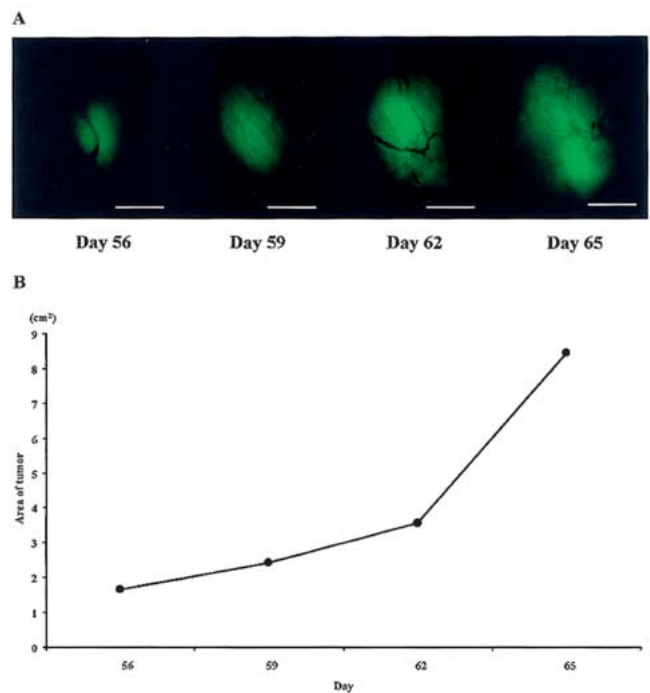


Table 1. HT-1080-GFP spontaneous lung metastasis in SCID mice.

Mouse #	Lung metastasis	Number of colonies
1	+	9
2	+	10
3	+	7
4	+	11
5	+	20
6	+	N.A.
7	+	13
8	+	8
9	+	N.A.
10	+	7
11	+	5
12	Still survive	–
	Mean	10.0
	SD	4.4

HT-1080-GFP cells (5×10^6) were injected in the right hind footpad of SCID mice (4 weeks old). Immediately after the death of each mouse, the lungs were removed and the number of GFP colonies were counted with a CCD camera (2 \times magnification).

Each week after cell injection, a skin-flap window was made for external imaging of lung metastasis. To make the skin-flap, the animals were anesthetized with a ketamine mixture (ketamine HCl 10 μ l, xylazine 7.6 μ l, acepromazine maleate 2.4 μ l, H₂O 10 μ l) via subcutaneous injection. An arc-shaped incision was made in the skin over the chest wall and subcutaneous connective tissue was separated to free the skin flap. The skin flap could be repeatedly opened each week to image tumor cells on the lung through the nearly transparent mouse chest wall. After external imaging (please see below), the skin-flap was simply closed with a 6-0 suture. The skin-flap window reduces the scatter of fluorescent photons [13].

Fluorescent optical imaging

Images were captured directly with a Hamamatsu C5810 3CCD camera (Hamamatsu Photonics, Bridgewater, New Jersey). For macro-imaging, a fluorescence light box (Lighttools Research, Encinitas, California) was used. For micro imaging, a Leica fluorescence stereo microscope model LZ12 was coupled with the CCD camera. This microscope was equipped with a GFP filter set and a mercury lamp with a 50-W power supply. Images were processed for contrast and brightness and analyzed with the use of Image ProPlus 3.1 software. 1024 \times 724 pixels high-resolution images were captured directly on an IBM PC.

All animal studies were conducted in accordance with the principles and procedures outlined in the National Institutes of Health Guide for the Care and Use of Laboratory Animals under assurance of number A3873-1.

Results and discussion

Properties of HT-1080-GFP *in vitro*

The selected HT-1080 cells have a strikingly bright GFP fluorescence *in vitro* (Figure 1). All cells in the population expressed GFP, indicating stability of the transgene (Figure 1). There was no difference in the doubling times of parental HT-1080 and selected HT-1080-GFP cells determined by comparison of proliferation rates in monolayer culture (data not shown).

Lung metastasis of HT-1080-GFP

Fluorescent metastasis on the lungs could be imaged through the skin six weeks after footpad injection (Figure 2A). However, clearer images were acquired by imaging through the skin-flap window (Figure 2B).

After sacrifice, multiple lung metastases were visualized by fluorescence imaging on the surface of the lung (Figures 3A and 3B). Macrometastasis on each side of the extracted lung were readily visualized by fluorescence microscopy (Figure 3C). The number of metastases on the lung surface was 10.0 ± 4.4 (mean \pm S.D., $n = 9$) (Table 1). Micrometastases consisting of a few cells were visualized on the surface of the extracted lung at 40 \times magnification (Figure 3D).

Real-time imaging of lung metastases

Twelve of 15 SCID mice (80%) had primary footpad tumors after HT-1080-GFP injection. In 11 of 12 mice (91.7%), lung metastases were visualized via the skin-flap window. Almost all mice survived 60 to 90 days after footpad injection (Figure 4). Lung micrometastases were visualized growing via skin-flap windows starting 8 weeks after injection at days 56, 59, 62, and day 65 (Figure 5A). These images were readily quantified by their area (Figure 5B). There were no visceral, bone, or soft tissue metastases observed.

In the present investigation, we used footpad injection of the human HT-1080 fibrosarcoma to obtain spontaneous lung metastasis in SCID mice [15–17]. The footpad has numerous fibrous tissues, which is where fibrosarcoma originates clinically [18, 19].

In the present study, lung metastases were visualized through the skin by whole-body fluorescence imaging (Figure 2A). However, to obtain higher resolution images, we used a skin-flap window [13]. All SCID mice survived multiple skin-flap procedures, enabling real-time imaging of spontaneous lung metastases in the same animal (Figure 2B). Image resolution via the skin-flap window was approximately 50–100 μ m allowing real-time imaging of micrometastasis formation (Figure 2B). Such capability will enable many experimental approaches not previously possible to investigate regulation of metastasis by genetic and physiological factors. External imaging is also an important improvement over sacrificing animals at each time-point to acquire averaged results in drug efficacy studies which now can be carried out in real-time.

Acknowledgement

This study was supported in part by the National Cancer Institute grant 1 R43 CA89779-01.

References

1. Tsuchiya H, Tomita K, Mori Y et al. Marginal excision for osteosarcoma with caffeine assisted chemotherapy. *Clin Orthop* 1999; 358: 27–35.
2. Tsuchiya H, Yamamoto N, Asada H et al. Caffeine-potentiated radiochemotherapy and function-saving surgery for high-grade soft tissue sarcoma. *Anticancer Res* 2000; 20: 2137–43.
3. Genoni M, Biraima AM, Bode B et al. Combined resection and adjuvant therapy improves prognosis of sarcomas of the pulmonary trunk. *J Cardiovasc Surg (Toronto)* 2001; 6: 829–33.
4. Wexler H. Accurate identification of experimental pulmonary metastasis. *J Natl Cancer Inst* 1966; 36: 641–5.
5. Chishima T, Miyagi Y, Wang X et al. Cancer invasion and micrometastasis visualized in live tissue by green fluorescent protein expression. *Cancer Res* 1997; 57: 2042–7.
6. Chishima T, Miyagi Y, Wang X et al. Visualization of the metastatic process by green fluorescent protein expression. *Anticancer Res* 1997; 17: 2377–84.
7. Chishima T, Miyagi Y, Wang X et al. Metastatic patterns of lung cancer visualized live and in process by green fluorescent protein expression. *Clin Exp Metastasis* 1997; 15: 547–52.
8. Chishima T, Miyagi Y, Li L et al. Use of histoculture and green fluorescent protein to visualize tumor cell host interaction. *In Vitro Cell Dev. Biol. Animal* 1997; 33: 745–7.
9. Yang M, Hasegawa S, Jiang P et al. Widespread skeletal metastatic potential of human lung cancer revealed by green fluorescent protein expression. *Cancer Res* 1998; 58: 4217–21.
10. Yang M, Jiang P, Sun FX et al. A fluorescent orthotopic bone metastasis model of human prostate cancer. *Cancer Res* 1999; 59: 781–6.
11. Yang M, Chishima T, Wang X et al. Multi-organ metastatic capability of Chinese hamster ovary cells revealed by green fluorescent protein (GFP) expression. *Clin Exp Metastasis* 1999; 17: 417–22.
12. Yang M, Baranov E, Jiang P et al. Whole-body optical imaging of green fluorescent protein-expressing tumors and metastases. *Proc Natl Acad Sci USA* 2000; 97: 1206–11.
13. Yang, M., Baranov, E., Wang, J-W. et al. Direct external imaging of nascent cancer, tumor progression, angiogenesis, and metastasis on internal organs in the fluorescent orthotopic model. *Proc Natl Acad Sci USA* 2002; 99: 3824–9.
14. Yang M, Jiang P, An Z et al. Genetically fluorescent melanoma bone and organ metastases models. *Clin Cancer Res* 1999; 5: 3549–59.
15. Matsumoto Y, Saiki I, Murata J et al. Recombinant human granulocyte colony-stimulating factor inhibits the metastasis of hematogenous and nonhematogenous tumors in mice. *Int J Cancer* 1991; 49: 444–9.
16. De Flora S, D'Agostini F, Masiello L et al. Synergism between N-acetylcysteine and doxorubicin in the prevention of tumorigenicity and metastasis in murine models. *Int J Cancer* 1996; 67: 842–8.
17. Ophir R, Moalem G, Pecht M et al. THF-gamma 2-mediated reduction of pulmonary metastases and augmentation of immunocompetence in C57BL/6 mice bearing B16-melanoma. *J Immunother* 1999; 22: 103–13.
18. Galinski AW, Russell SC, Krause, R. Fibrosarcoma of the foot. A case report. *J Am Podiatry Assoc* 1981; 71: 631–3.
19. Blume PA, Niemi WJ, Courtright DJ, Gorecki GA. Fibrosarcoma of the foot: A case presentation and review of the literature. *J Foot Ankle Surg* 1997; 36: 51–4.